

## 2+1 Flavor Domain Wall Fermion QCD Lattices: Ensemble Production and (some) Properties

---

**Robert D. Mawhinney**<sup>\*†</sup>

*Columbia University*

*The RBC and UKQCD Collaborations*

*E-mail:* [rdm10@columbia.edu](mailto:rdm10@columbia.edu)

The RBC and UKQCD Collaborations continue to produce 2+1 flavor domain wall fermion ensembles, currently focusing on an ensemble with a  $96^3 \times 192$  volume on SUMMIT at ORNL with  $1/a \approx 2.8$  GeV, and smaller ensembles at stronger couplings. The  $1/a \approx 2.8$  GeV ensemble uses the Exact One Flavor Algorithm for the strange quark, along with the Multisplitting Preconditioned Conjugate Gradient for solving the Dirac equation. We report on our progress and experience to date with the evolution of this ensemble.

*37th International Symposium on Lattice Field Theory - Lattice2019*

*16-22 June 2019*

*Wuhan, China*

---

<sup>\*</sup>Speaker.

<sup>†</sup>This work was done in collaboration with members of the RBC and UKQCD Collaborations, with major contributions from Chulwoo Jung, David Murphy and Jiqun Tu. Substantial support for the implementation in QUDA of some of the algorithms discussed here was provided by Kate Clark of Nvidia. Time on the Summit computer at ORNL was provided through DOE INCITE award PHY131 in 2019. MSPCG algorithm development and algorithm tuning on the small volume was done on Mira at the ALCF. This research used resources of the Oak Ridge Leadership Computing Facility at the Oak Ridge National Laboratory, which is supported by the Office of Science of the U.S. Department of Energy under Contract No. DE-AC05-00OR22725. This research used resources of the Argonne Leadership Computing Facility, which is a DOE Office of Science User Facility supported under Contract DE-AC02-06CH11357. The author is supported in part by U.S. DOE grant #DE-SC0011941.

## 1. Introduction

The RBC and UKQCD Collaborations have been generating 2+1 flavor Domain Wall Fermion (DWF) and Mobius Domain Wall Fermion (MDWF) ensembles since 2005. A complete list of these ensembles, with the Iwasaki gauge action, is given in Table 1. These have been used for measurements for many different QCD observables, including kaon decays, measurements of LECs for chiral perturbation theory, the hadron vacuum polarization and hadronic light-by-light scattering for  $g - 2$  of the muon, and the  $K_L - K_S$  mass difference. (We note that another set of 2+1 flavor ensembles, with the Iwasaki + Dislocation Suppressing Determinant Ratio (DSDR) gauge action is also available. The presence of the DSDR term allows for simulations at larger lattice spacings, while still allowing the residual mass to be kept small for accessible values of the fifth dimension,  $L_s$ , of (M)DWF.)

For the last 5 years, 2 ensembles with spatial volumes greater than  $(5.4 \text{ fm})^3$  and essentially physical pion and kaon masses have been available [1]. These are shown in the first two red rows in Table 1. Combining these ensembles at two lattice spacings with a third Iwasaki plus DSDR ensemble, and requiring a common continuum limit for observables, has shown that the  $\mathcal{O}(a^2)$  scaling errors are modest and that, within our statistics, only  $\mathcal{O}(a^2)$  correction terms are needed.

However, for any observables dependent on the valence charm quark mass, the coarsest Iwasaki action ensemble ( $1/a = 1.730 \text{ GeV}$ ) and the Iwasaki+DSDR ensemble ( $1/a = 1.35 \text{ GeV}$ ) are too coarse to be of use, even for simulations with  $m_c$  lighter than its physical value, where an eventual extrapolation to the physical  $m_c$  value is done. For access to charm quark physics, a smaller lattice spacing is needed to augment the  $1/a = 2.359 \text{ GeV}$  ensemble. Such an ensemble was produced, with  $1/a = 2.774 \text{ GeV}$ ,  $m_\pi = 234 \text{ MeV}$  and a  $(3.5 \text{ fm})^3$  spatial volume [2]. In spite of the smaller lattice spacing, reasonable topological tunneling was observed for this ensemble with current algorithms. Given this success, we have begun the production of an ensemble with this lattice spacing, physical pion mass and a larger volume. This ensemble's properties (expected from our global chiral perturbation theory fits to all of our other ensembles) are shown in the last red row of Table 1. The ongoing production of lattices in this ensemble is the subject of this report.

## 2. Using The Exact One Flavor Algorithm

Using standard pseudofermion methods to represent the determinant of a single quark flavor has been possible for many years, with the advent of the Rational Hybrid Monte Carlo (RHMC) algorithm. Generically,  $\det(D)$ , which represents a single flavor must be changed to  $\det(D^\dagger D)$ , which represents two flavors, in order to have an operator with a positive definite spectrum which is suitable for representation by non-Grassmanian (bosonic) pseudofermion fields. To get back to the correct determinant factor for a single flavor, one needs to use pseudofermions to represent  $\det([D^\dagger D]^{1/2})$ . The RHMC algorithm uses a rational function representation to accurately represent the square root function over the spectral range of the eigenvalues of  $D^\dagger D$ .

While the RHMC has been very successful, the single quark flavor (strange) that it implements in modern (M)DWF simulations has become computationally costly, in spite of the large value of the strange quark mass in comparison to the degenerate light quark masses. There are two primary reasons for this. First, while the required Dirac equation solves for the RHMC can be performed

Action	$1/a$	Lattice	$m_l$	$m_s$	$m_{\text{res}}$	$m_\pi$	$m_K$	Size
(F+G)	(GeV)	volume	(in lattice units)			(MeV)	(MeV)	(fm)
DWF+I	1.785(5)	$24^3 \times 64 \times 16$	0.03	0.04	0.00308	693		2.6
DWF+I	1.785(5)	$24^3 \times 64 \times 16$	0.02	0.04	0.00308	576		2.6
DWF+I	1.785(5)	$24^3 \times 64 \times 16$	0.01	0.04	0.00308	432	626	2.6
DWF+I	1.785(5)	$24^3 \times 64 \times 16$	0.005	0.04	0.00308	340	593	2.6
<b>MDWF+I</b>	<b>1.730(4)</b>	<b><math>48^3 \times 96 \times 24</math></b>	<b>0.00078</b>	<b>0.0362</b>	<b>0.000614</b>	<b>139</b>	<b>499</b>	<b>5.5</b>
DWF+I	2.383(9)	$32^3 \times 64 \times 16$	0.008	0.03	0.000664	412	615	2.6
DWF+I	2.383(9)	$32^3 \times 64 \times 16$	0.006	0.03	0.000664	360	596	2.6
DWF+I	2.383(9)	$32^3 \times 64 \times 16$	0.004	0.03	0.000664	302	579	2.6
<b>MDWF+I</b>	<b>2.359(7)</b>	<b><math>64^3 \times 128 \times 12</math></b>	<b>0.000678</b>	<b>0.02661</b>	<b>0.000314</b>	<b>139</b>	<b>508</b>	<b>5.4</b>
MDWF+I	2.774(10)	$48^3 \times 96 \times 12$	0.002144	0.02144	0.000229	234	516	3.5
<b>MDWF+I</b>	<b>2.774(10)</b>	<b><math>96^3 \times 192 \times 12</math></b>	<b>0.000541</b>	<b>0.0213</b>	<b>0.000229</b>	<b>135</b>	<b>495</b>	<b>6.9</b>
DWF+I	3.15(2)	$32^3 \times 64 \times 12$	0.0047	0.0186	0.000631	371	558	2.0

**Table 1:** A summary of the 2+1 flavor (M)DWF ensembles generated by the RBC and UKQCD Collaborations. All ensembles use the Iwasaki gauge action. The three ensembles highlighted in red have essentially physical pion and kaon masses and spatial volumes greater than  $(5.4 \text{ fm})^3$ . This report focuses on the ongoing production of the  $96^3 \times 192 \times 12$  ensemble with  $1/a = 2.774(10)$  GeV.

with a multi-shift conjugate gradient algorithm, this solver is not restartable, so it is difficult to run in lower precision. Since modern CPUs and GPUs are memory bandwidth limited and have high-performance, reduced precision floating point units, there is a substantial performance penalty for running the conjugate gradient (CG) partly or largely in double precision. Secondly, for (M)DWF, adding Hasenbusch preconditioning masses, *i.e.*  $\det([D^\dagger(m_1)D(m_1)]^{1/2})/\det([D^\dagger(m_2)D(m_2)]^{1/2})$  is expensive, since the  $1/2$  power of the Dirac operators appearing in the denominator must be implemented as two,  $1/4$  power operators to preserve reversibility of the algorithm. From the light quark sector, it is well known that Hasenbusch preconditioning is important in balancing the size of the fermionic force the integrator must handle with the expense of calculating that force. The lack of Hasenbusch preconditioners for the RHMC part of the algorithm increases the expense of this part of the simulation.

Fortunately, an alternative to the RHMC, the Exact One Flavor Algorithm (EOFA) has been proposed in [3] and shows that

$$\det \left[ \frac{D_{DWF}(m_1)}{D_{DWF}(m_2)} \right] = \frac{1}{\det \mathcal{M}_L} \frac{1}{\det \mathcal{M}_R} \quad (2.1)$$

with  $\mathcal{M}_L$  and  $\mathcal{M}_R$  Hermitian and positive definite. We have tested and implemented this algorithm as detailed in [4] and have found that the Dirac equation solution needed for the EOFA system can be recast into an appropriate solve for a (M)DWF system. This allows us to reuse the existing (M)DWF

high performance solver code for the EOFA system. (For our G-parity simulations with MDWF, the EOFA has been extremely beneficial, since here the  $1/2$  power of the light quark determinant is needed. By adding in Hasenbusch preconditioning masses, being able to solve in single precision with defect correction restarts and retuning the parameters for the HMC, we achieved a  $4.5\times$  wall clock speed up over our earlier RHMC implementation.)

For the evolution of our current  $96^3 \times 192 \times 12$  ensemble with  $1/a = 2.774(10)$  GeV on Summit, we have implemented the EOFA algorithm on GPUs. In particular, the pseudofermion heat-bath for the EOFA algorithm does require a rational approximation to a fractional power of the EOFA operator. (We stress that this is only in the initial heat-bath part of a molecular dynamics trajectory.) Implementation of this heat bath in QUDA was done by David Murphy. The QUDA Mobius Dirac operator code had to be generalized to implement the generic EOFA linear system and this was done by Jiqun Tu. Kate Clark of Nvidia provided invaluable advice and support in these implementations.

### 3. Algorithm Tuning

In preparation for the generation of our  $96^3 \times 192 \times 12$  ensemble on Summit, we thermalized a  $32^3 \times 64 \times 12$  ensemble on Mira, with the same input quark masses and couplings. This smaller ensemble has too small a volume,  $(2.3 \text{ fm})^3$ , for sensible physics results, but for tuning algorithm parameters and comparing the results with the RHMC and EOFA algorithms, it is expected to be a reliable testing ground.

Tuning of the HMC algorithm involves making choices for the Hasenbusch masses, choosing the conjugate gradient stopping condition for each required Dirac equation solve, choosing the accuracy for the conjugate gradient solves needed to calculate the initial and final values for the Hamiltonian and choosing the step size to achieve the desired acceptance (usually around 90%). Most of these choices cannot be made until one has reasonably thermalized the ensemble, since, for example, the fermion force due to each Hasenbusch mass ratio generically depends on the thermalization. In order to proceed, we start with a reasonable set of guesses for these parameters and let the ensemble begin to thermalize. Given the much lower calculational cost for the smaller volume, it is much easier to begin these tunings on this system.

We have found that the choice of Hasenbusch masses can be guided by monitoring the L-infinity norm of  $F \cdot dt$  over the entire lattice for each step in the molecular dynamics. Here  $F$  is the fermionic force from a particular Hasenbusch determinant ratio and we plot histograms of these L-infinity norms for some number of trajectories. (Detailed examples of these tunings are given in [4].) Adding more Hasenbusch masses decreases the overall force, but there is a cost to each additional mass. We also find that the acceptance decreases when there are occasional large forces and that these fluctuations in forces are more pronounced for the Hasenbusch ratios for the lightest quarks.

Our input light quark mass should be 0.000541 which adds to the expected residual mass of 0.000229 to give a total light quark mass of 0.000770. (The residual mass value comes from the  $1/a = 2.744$  GeV ensemble with a 234 MeV pion. This is our best estimate for this and since the residual mass has mild dependence on the input light quark mass, we expect this to be reliable.) From the small volume ensemble running, after thermalizing for many hundreds of trajectories

and experimenting with different Hasenbusch choices, we gathered 56 trajectories of data with intermediate Hasenbusch masses of 0.0056, 0.028, 0.1, 0.28, 0.56. The forces from the determinant ratios containing the masses (0.000541,0.0056) and (0.028, 0.1) showed occasional large fermionic forces almost twice as large as the largest values from other determinant ratios.

At this point, our Summit code was ready to run and the machine was available, so we replicated our  $32^3 \times 64 \times 12$  thermalized lattice 3 times in each space-time direction (81 copies overall) and began evolution of a  $96^3 \times 192 \times 12$  ensemble on Summit. Clearly, substantial thermalization time is needed for the large ensemble to eliminate the replications, but we can continue our algorithm tuning during this time and the tunings should be more reliable than tuning on an ensemble which has not been equilibrated at all.

Figure 1 shows a histogram of the L-infinity norm of  $F \cdot dt$  for 10 trajectories on the  $96^3 \times 192 \times 12$  ensemble after about 300 trajectories of thermalization on the large volume after it was made by replicating the small volume. An additional intermediate Hasenbusch mass has been added and one can see that the occurrence of large forces is fairly similar for all of the Hasenbusch mass ratios. One sees that the lightest mass produces somewhat more large forces than the others. The figure also shows the forces due to an intermediate Hasenbusch mass used in the EOFA algorithm. One clearly sees that to keep the EOFA forces in agreement with the light quark forces, an intermediate mass of 0.163 has been added. Without the addition of this mass, the single-flavor strange quark forces would be larger than those from any of the individual light-quark Hasenbusch ratios.

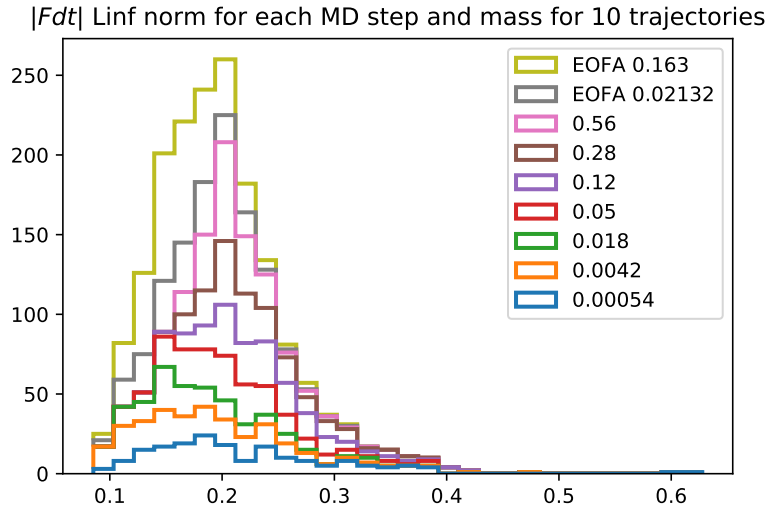


**Figure 1:** A histogram of the L-infinity norm of  $F \cdot dt$  for the  $96^3 \times 192 \times 12$  ensemble for 10 trajectories around trajectory 300. The number labeling a color is the quark mass appearing in the numerator of the Hasenbusch mass ratio. Unless explicitly labeled EOFA, the forces are for the light quarks.

Another test done on the small volume ensemble was to compare the speed with the RHMC and EOFA algorithms. With one choice of Hasenbusch masses, and all other parameters held the same, just replacing the RHMC with the EOFA decreased the time per trajectory by 30%. The

overall speed up is expected to be much larger, as is evident in Figure 1, since the EOFA forces are now in line with the light-quark forces. We have not tried running any RHMC comparison tests for the  $96^3 \times 192 \times 12$  ensemble, given the costs of such a test and the need to keep acceptances the same to fully understand the wall clock time differences.

#### 4. The Multisplitting Preconditioned Conjugate Gradient (MSPCG)

The Summit computer, with 6 Nvidia V100 GPUs per node, has extensive on-node floating point power (42 TFlops, double precision), but only a 100 GB/s Mellanox link providing network bandwidth between nodes. This is very little bandwidth for strong scaling the solvers used for DWF QCD to, say, 1024 nodes, since the local volumes implied by a 1024 node job generally require of order one byte of off-node bandwidth per sustained Flop. To increase local (on-node) floating point utilization in the (M)DWF conjugate gradient, we have developed the Multisplitting Preconditioned Conjugate Gradient (MSPCG) [5, 6]. The Multisplitting algorithm [7] provides general criteria for detailing how a linear equation solve can be split into submatrix pieces, with each solved separately, and then an update step is done, which spans the submatrices, to redefine the next iteration of the problem.

While investigating this method for the preconditioned normal (M)DWF operator

$$D_{PC}^\dagger D_{PC} = [M_5 - M_e^4 M_5^{-1} M_{eo}^4]^\dagger [M_5 - M_e^4 M_5^{-1} M_{oe}^4]^\dagger \quad (4.1)$$

which connects fourth nearest-neighbor sites on the lattice (see [5, 6]) we originally failed to get convergence. Our initial approach split the underlying four-dimensional Wilson Dirac operator ( $M_4$ ) into submatrices localized on each GPU, *i.e.* we tried to split the parts of  $D_{PC}^\dagger D_{PC}$  into submatrices rather than splitting  $D_{PC}^\dagger D_{PC}$  into submatrices. Changing so that we were splitting  $D_{PC}^\dagger D_{PC}$  into submatrices made the Multisplitting algorithm converge, but it converged more slowly than the original CG. However, we were able to use the local submatrix decomposition as a preconditioner to the CG and found that the CG iteration count fell by a factor of 3 for physical light quark masses [5]. (Using the multisplitting algorithm as a preconditioner for the CG, when the submatrix decomposition is the natural one given by the underlying lattice geometry, makes our implementation the same as using the additive Schwarz algorithm as a preconditioner.)

For our ensemble generation on Summit, the speed-up possible with the MSPCG depends on the performance that can be achieved for a strictly local linear equation solve on each V100. If these local solves were infinitely fast, *i.e.* the preconditioner took no time, our evolution would speed up by almost a factor of 3. The preconditioner allows us to trade local floating point power for network bandwidth.

Jiqun Tu has implemented the preconditioner in the QUDA CG, with support and consultation provided by Kate Clark of Nvidia. Despite their large floating point speed, the memory bandwidth of the V100s limits their performance and hence the speed of the preconditioner. Tu's implementation of the preconditioner has also utilized the tensor cores on the V100. These are very efficient for dense matrix multiply and the fifth-dimensional part of (M)DWF does contain a substantial amount of dense matrix arithmetic. By fusing kernels to keep data in the device memory, Tu's implementation is able to see a performance boost through the use of the tensor cores.



Table 2 summarizes the performance of the MSPCG on the target  $96^3 \times 192 \times 12$  ensemble for various numbers of nodes and CG steps for the preconditioner. One important item to note is that, for the 1024 node case, the standard CG runs at 2.93 TFlops/node, which is about 2 times faster than the performance when Summit first came on line. This reflects optimizations and improvements in the Summit software stack. For this same 1024 node case, MSPCG gives a speed-up of 1.22, which is an important, but modest gain. If the outer CG was running at its original slower speed, the gain from the MSPCG would be much larger.

nodes	local volume	solver	inner iter.	(outer) iter.	r.u.	performance/node	time	speed up
256	16 · 24 · 12 · 24	CG	–	42133	471	4.66	486.3	1.10x
		MSPCG	05	16903	195	1.56(01)/5.45(35)/37.29(53)	456.0	
		MSPCG	06	14860	173	1.56(01)/5.51(31)/37.60(58)	442.6	
		MSPCG	07	13787	161	1.56(01)/5.48(28)/37.49(60)	460.2	
		MSPCG	08	12922	151	1.56(01)/5.44(26)/37.55(63)	469.5	
512	16 · 12 · 12 · 24	CG	–	42427	474	3.85	296.6	1.13x
		MSPCG	05	17625	203	1.26(01)/4.54(37)/36.21(52)	271.0	
		MSPCG	06	15425	179	1.27(01)/4.55(33)/36.26(57)	262.1	
		MSPCG	07	14409	168	1.26(01)/4.57(30)/36.39(60)	268.3	
		MSPCG	08	13597	159	1.27(01)/4.53(28)/36.35(63)	276.0	
1024	16 · 12 · 12 · 12	CG	–	42482	474	2.93	195.2	1.22x
		MSPCG	05	18250	210	1.00(01)/3.68(34)/34.62(45)	183.3	
		MSPCG	06	15959	185	1.01(01)/3.68(35)/34.79(54)	159.7	
		MSPCG	07	14985	174	1.01(01)/3.68(32)/35.06(58)	163.6	
		MSPCG	08	14287	167	1.00(01)/3.69(29)/34.76(61)	169.1	

**Table 2:** Strong scaling of the MSPCG on SUMMIT for solving the Dirac equation  $D_{PC}^\dagger D_{PC} x = y$  to the accuracy of  $10^{-12}$  on the  $96^3 \times 192 \times 12$ , 2+1 flavor Möbius domain wall fermion,  $1/a = 2.774$  GeV lattice with physical pion mass. Here  $y$  is a gaussian random source vector and the MSPCG is implemented within the QUDA software environment. The times are time-to-solution given in units of seconds. The column titled "r.u." denotes the number of reliable updates performed. In the "performance/node" column, the performance is given in tera-flops per node, with the percentage of time spent in a particular part of the algorithm given in parentheses. For the CG solver the performance is given as the total performance, including precise and sloppy dslash and linear algebra operations. For MSPCG solves the performance is given in the format of precise/sloppy/preconditioned dslash with their respective time percentages in parentheses. The purple background highlights the best MSPCG result for a given number of nodes. (This table is reproduced from the Ph.D. thesis of Jiqun Tu, Columbia University, 2019.)

## 5. Ongoing Evolution of the Ensemble

As of late December, 2019, we have produced 730 unit length trajectories for the  $96^3 \times 192 \times 12$  ensemble on Summit. With Chulwoo Jung integrating the QUDA enabled versions of the MSPCG and EOFA algorithm into the Columbia Physics System and managing the production running, he was able to refine the choices of Hasenbusch masses during the first few hundred trajectories. Even after around 200 trajectories, when the lattice should have been close to thermalized, he noticed that  $\langle \exp(-\Delta H) \rangle$  was not averaging to one, with occasional large values,  $\mathcal{O}(20)$ , appearing. We adjusted the number of poles in the rational approximation needed in the EOFA heat bath, and tightened the stopping condition for the solvers calculating this part of the Hamiltonian, and the occasional outliers have gone away. In particular for trajectories 300 to 730,

$\langle \exp(-\Delta H) \rangle = 0.94(5)$ , where the error comes from assuming that values of  $\Delta H$  are decorrelated for each trajectory.

An important quantity is the evolution of global topological charge,  $Q_{top}$ , which is shown in Figure 2. From this figure, one can see substantial excursions in  $Q_{top}$  that take  $\mathcal{O}(200)$  molecular dynamics time units. The histogram of topology shows it is not symmetric around zero, with a current bias towards positive values. This figure indicates that we are far from a situation with frozen  $Q_{top}$  and we anticipate running with longer molecular dynamics trajectories to further speed up the evolutions of topological charge.

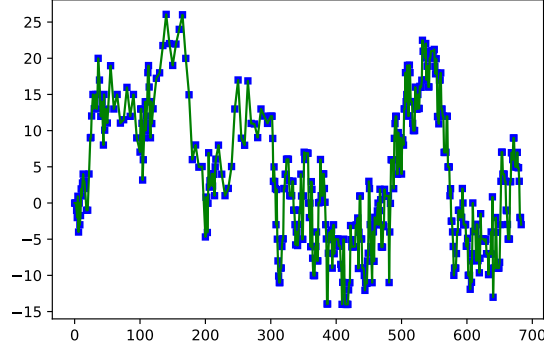


**Figure 2:** The evolution of topological charge for the  $96^3 \times 192 \times 12$  ensemble. The horizontal axis is in molecular dynamics time units and for us one trajectory is one molecular dynamics time unit.

## 6. Conclusions

We have a successfully evolved a  $96^3 \times 192 \times 12$ , 2+1 flavor, (M)DWF ensemble for 730 molecular dynamics time units on the Summit computer at ORNL. This ensemble has  $1/a = 2.774$  GeV and a spatial volume of  $(6.9 \text{ fm})^3$ . The evolution has been done on partition sizes of 256, 512 and 1024 nodes. We see reasonable evolution of topological charge and are expecting to move to longer molecular dynamics trajectory lengths to improve topological charge evolutions.

## References

- [1] T. Blum, *et. al.*, Phys. Rev. D93 (2016) 074505, arXiv:1411.7017 [hep-lat].
- [2] Peter A. Boyle, *et. al.*, JHEP 1712 (2017) 008, arXiv:1701.02644 [hep-lat].
- [3] Y.-C. Chen and T.-W. Chiu (TWQCD), Phys. Lett. B738, 55 (2014), arXiv:1403.1683 [hep-lat].
- [4] C. Jung, C. Kelly, R.D. Mawhinney and D.J. Murphy, Phys. Rev. D97 (2018) 054503, arXiv:1706.05843 [hep-lat].
- [5] D. Guo, R. Mawhinney and J. Tu, arXiv:1804.08593 [hep-lat].
- [6] Jiqun Tu, arXiv:1811.08488 [hep-lat], PoS LATTICE2018 (2018) 030.
- [7] D.P. O’Leary and R.E. White, SIAM J. Algebr. Discret. Methods 6, 630 (1985).